Submitted to small

DOI: 10.1002/smll.((please add manuscript number))

High concentration solvent-exfoliation of graphene

By *Umar Khan, Arlene O'Neill, Mustafa Lotya, Sukanta De,* and *Jonathan N Coleman* *

[*] Prof. J. N. Coleman, Dr. S. De, Dr U. Khan, Mr M. Lotya, Ms. A. O'Neill
School of Physics and CRANN
Trinity College Dublin,
Dublin 2 (Ireland)
E-mail: (colemaj@tcd.ie)

Keywords: (graphene, solvent, dispersion, exfoliation, films)

We demonstrate a method to prepare graphene dispersions at high concentrations, up to 1.2 mg/ml, with yields of up to 4wt% monolayers. This process relies on low-power sonication for long times, up to 460 hours. TEM shows the sonication to reduce the flake size with flake dimensions scaling as $t^{-1/2}$. However, the mean flake length remains above 1 μm for all sonication times studied. Raman spectroscopy shows defects are introduced by the sonication process. However, detailed analysis suggests that predominately edge rather then basal-plane defects are introduced. We have used these dispersions to prepare high quality free-standing graphene films. The dispersions can be heavily diluted by water without sedimentation or aggregation. This method facilitates graphene processing for a range of applications.

1.0 Introduction

The unprecedented mechanical[1], electrical[2] and thermal properties[3] of graphene have sparked huge interest among researchers in recent years[4, 5]. While many of the ground-breaking experiments have been carried out on micromechanically cleaved monolayers[6], future industrial applications are likely to require large-scale, high-throughput processing methods[7]. Early progress in this area involved the oxidisation of graphite, followed by exfoliation in water, to give aqueous dispersions of graphene oxide (GO).[8, 9] This material consists of sp^2 bonded carbon sheets decorated with large numbers of covalently attached hydroxyl and epoxide groups. The polar nature of these groups, coupled with the Coulomb repulsion associated with extensive proton dissociation[10], means that these dispersed GO sheets are very stable in aqueous environments. Such dispersions are very useful as they facilitate both materials processing and fundamental characterisation. For example, they have been used to deposit individual sheets for spectroscopic analysis[11, 12], prepare polymer-graphene composites[8] and develop graphene thin-films[13, 14].

However, GO faces some significant disadvantages. Due to the disruption in the π-orbital structure on oxidisation, GO is a poor electrical conductor[15]. The oxides can be removed by thermal or chemical reduction resulting in a significant increase in conductivity [15-17]. However, reduction adds yet another step in the processing procedure. In addition, thermal reduction is most successfully carried out at ~1000C,[13, 18, 19] a temperature which is unsuitable for many applications. Moreover, reduction cannot remove the many structural defects introduced by the oxidation process.[15, 20-24] These defects disrupt the band structure and completely degrade the electronic properties which make graphene unique.

In order to address these issues, our group[25, 26] and others[27-29] have developed methods to exfoliate powdered graphite to give graphene in the liquid phase without oxidation or defect formation. These methods rely on the exfoliation and stabilisation of graphene using special solvents or surfactants and suffer from none of the problems outlined above. As such, solvent or surfactant exfoliated graphene has the potential to be useful in a host of applications in both research and industry. However, these methods have one critical disadvantage: The graphene can only be dispersed at relatively low concentration, typically <0.01 mg ml^{-1}. Such a low concentration makes many applications completely impractical. This gives graphene oxide a significant advantage as it can be dispersed in some organic solvents at concentrations of up to 1 mg ml^{-1},[15, 30-32] and in water at concentrations of up to 7 mg ml^{-1}.[33]

In order to gain full advantage from dispersions of pristine graphene in solvents, it will be critical to increase the maximum concentration obtainable while maintaining the quality of the graphene flakes. In this work we demonstrate such a method. We show that by applying mild sonication for long times (up to 460 hours) in the solvent N-methyl-pyrrolidone (NMP), we can increase the graphene concentration to ~1 mg ml^{-1}. We use TEM analysis to show that the dispersions almost exclusively contain flakes with less than 10 layers. For the sample sonicated for 100 hrs, over 90% of flakes had less than 5 layers. Raman spectroscopy suggests that minimal quantities of basal plane defects are introduced. Finally we show that these dispersions can be used to prepare films with reasonable electrical and mechanical properties.

2.0 Results and Discussion

2.1 Graphene concentration as a function of sonication time

We hypothesised that the concentration of exfoliated graphene dispersed in solvents such as N-methyl-pyrrolidone is limited by the amount of energy added during the sample preparation process. This can be tested by monitoring the dispersion quality (dispersed concentration, flake size & thickness etc) as a function of sonication time. A large quantity of graphene dispersion was bath sonicated (3.3 mg ml^{-1} graphite in 700 ml NMP, round bottomed flask) for 460 hours. At various times during this period, aliquots were removed for centrifugation (500 rpm) and subsequent analysis. The set of centrifuged dispersions appeared darker in colour for longer sonication times as shown in **figure 1**, upper inset. In all cases, the UV-vis absorbance spectra were measured, appearing flat and featureless[25]. The absorbance per cell length, A/l, of these dispersions (660 nm) is plotted versus sonication time in figure 1. The concentration remaining after centrifugation, C_G, can be measured from A/l once the absorption coefficient, α, is known ($A = \alpha C_G l$). We measured α (660 nm) for a range of sonication times and centrifugation rates by preparing large volumes of dispersion, measuring A/l, and then finding the dispersed mass by filtration and weighing. The absorption coefficient was relatively invariant with processing procedure (figure S1), displaying a mean value of α=3620 ml mg^{-1} m^{-1}, slightly higher than our previous estimate of α=2460 ml mg^{-1} m^{-1}.[25] The calculated concentration is shown on the right axis of figure 1. The concentration increased steadily with sonication time from 0.06 mg ml^{-1} after 0.5 hrs before saturating at 1.2 mg ml^{-1} after 270 hrs as shown in figure 1.This value is much larger than our previous maximum concentration (0.01 mg ml^{-1}) and is comparable to the best results for GO in organic solvents[34]. We note that empirically, this data closely follows $C_G \propto \sqrt{t}$.

At this point, it is important to comment on the sonication process. We have used bath sonication (see Experimental section for details), even though the sonication times are very long. This is because preliminary research in our group showed that intense tip sonication was relatively ineffective at exfoliating graphene from graphite. Since we finished these experiments, a paper has appeared which describes exfoliation of graphite to give graphene in surfactant solutions.[29] In this work, intense tip sonication was used successfully. In the future, it would be worthwhile to attempt to exfoliate graphene in solvents using tip sonication. The advantage of this would be that exfoliation could be achieved in much shorter times than those used here. When using sonic baths, another problem is reproducibility. This is because the sonic energy input to the sample is sensitive to the water level, the exact position in the bath, the volume of dispersion, vessel shape etc. In addition, sonic baths often have power outputs different to the rated power output (see Experimental section). As a result, nominally identically baths tend to give different results. Due to this equipment related variability, the concentration attained at any sonication time can vary by a factor of ~2 from the presented data. For example, after ~200 hours sonication we have obtained samples with concentration varying from ~0.5 mg/ml to ~1.5 mg/ml depending on the bath used. For this reason, all presented time-dependent measurements were made using the same stock, sonicated in a fixed position in one sonic bath. We also note that sonication for long times results in stabilisation of bath temperature at elevated levels, leading to water evaporation. A siphon system must be installed to keep the water level constant. In high power baths the steady state temperature can be greater than 50C, in some cases resulting in solvent degradation. As a result we tried to work at bath power outputs below 25 W.

2.2 Degree of exfoliation

Increasing the concentration of these dispersions is only useful if dispersion quality is maintained at the higher concentrations. To test this we carried out TEM analysis on a subset of dispersions. A few drops, taken from dispersions sonicated for 36, 96, 192 and 343 hrs, were dropped on holey carbon grids and analysed using TEM. Shown in **figure 2** are representative TEM images of the flakes observed. Figure 2A shows a graphene monolayer while figures 2 B&C show a multilayer. The monolayer can easily be identified by its well defined edges while the multilayer is typical of the larger objects observed regularly. We note that some very thick multilayers are observed on rare occasions. These objects are non-transparent to the electron beam but have lateral dimensions similar to the thinner flakes. Of >400 flakes observed, only 2 were such very thick objects. We note that for short sonication

times, the grids are sparsely coated by flakes, making them difficult to find by TEM. Shown in figure 2D is a wide-field image of a TEM grid prepared from a long sonication time sample (180 hrs). This image is covered by large numbers of flakes and is typical of those observed for longer sonication times. The larger numbers of flakes observed make statistical analysis relatively easy for these samples.

We can use TEM images of the type shown in figure 2 to generate statistical data on the exfoliation state of the graphene in these dispersions. We measure the lateral dimensions of large number of flakes per sample (typically ~100). In general, the flakes are irregularly shaped, so we measure the dimension along the long axis and designate this as the length, L. We designate the dimension perpendicular to the long axis as the width, w. In addition, we estimate the number of layers per flake, N, by examining the edges of the flakes. In TEM images of graphene multilayers, the edges of the individual flakes are almost always distinguishable. For example, the image in figure 2C is a magnification of the portion of figure 2B surrounded by the dashed box. Here five layer edges can clearly be seen (see arrows), showing this flake to be a 5-layer. Thus, by carefully counting the flake edges, it is possible to measure the number of layers per flake. We accept that for some multilayers, it is difficult to count the number of edges exactly. In such cases, only estimation of N is possible. However, we expect the errors involved to be random and so cancel out when data for many flakes are combined in a histogram. Using the edge-counting method, it is particularly easy to identify mono-layers. We previously demonstrated the effectiveness of monolayer identification in a previous publication by confirming their identification by edge counting with electron diffraction data.[25] As before we can confirm the identification of monolayers by analysis of electron diffraction patterns such as that shown in figure 1A inset. That the inner spots are more intense than the outer spots is definitive confirmation that the flake consists of one layer only.[25]

We analyse approximately 100 flakes for each sonication time. The full results of the flake thickness, length, width and aspect ratio (L/w) results are shown in supplementary information, figure S2-5 respectively. (We note that most researchers use Atomic Force Microscopy to measure flake thickness. However this is not possible here. Due to the high boiling point of most successful graphene solvents, flakes tend to aggregate during deposition onto surfaces, rendering quantitative AFM analysis impossible). We acknowledge that one problem with statistical analysis of TEM images is that some small flakes may be lost through the holes in the TEM grid. This would result in over-estimation of lateral flake size. However,

the agreement between predicted and measured data in figure 1 suggests that our flake size stats are reasonably accurate.

Shown in **figure 3A** is a histogram showing the distribution of flake thicknesses for the 343 hrs sample which had C_G=1.2 mg ml^{-1}. Even at this high concentration, the graphene is highly exfoliated. In figure 3B-D, we show $\langle N \rangle$, $\langle L \rangle$ and $\langle w \rangle$ as a function of sonication time as calculated from the distributions in figures S2-4. The mean number of layers per flake $\langle N \rangle$ is close to 3 for all sonication times. However, the lateral dimensions of each flake decreased significantly with sonication time, with the mean length falling from ~3μm to ~1μm and the mean width falling from ~1 μm to ~300 nm. The data for both flake length and width scale well with the inverse square root of time: $\langle L \rangle \propto t^{-1/2}$ and $\langle w \rangle \propto t^{-1/2}$. This behaviour was previously observed for carbon nanotubes and is expected theoretically.[35] We note that this time dependence explains a number of aspects of the data outlined below.

Additional statistics relating to the degree of exfoliation and flake dimensions as a function of sonication time are shown in figure S6. The mean flake aspect ratio, $\langle L/w \rangle$ was constant at 2.5-3 for all sonication times. That $\langle L/w \rangle \neq 1$ suggests that the exfoliation/cutting process favours asymmetric flakes. From the data in figure S2, we found that the fraction of flakes with <5 layers, $N_{1\text{-}4}/N_T$, was roughly constant between 80% and 90% for all samples. In addition, the fraction of monolayers, N_1/N_T, increased from ~10% for the short sonication times to 21% for the 343 hr sample. A monolayer fraction of 21% corresponds to a mass fraction of 7% (see *[25]* for details). Accounting for the fall-out during sedimentation, we can calculate a yield of 4% monolayer mass relative to the starting mass of graphite. This is significantly larger than the early values of <1%.[25]

2.3 Correlation of concentration and flake size

We suggest that the increase in graphene concentration is correlated with the decrease in flake dimensions as sonication time is increased. For dispersions of nanotubes in NMP, the equilibrium bundle diameter is set by the concentration, such that the total volume of solvent per bundle is proportional to the volume of the sphere whose diameter equals the bundle length (see figure 1, lower inset, left).[36] The physical basis of this is that when the bundles are brought closer, say by debundling, collisions can occur between diffusively rotating adjacent bundles resulting in aggregation. Given that nanotubes in NMP can spontaneously split from the bundles by desorption,[37] this results in a dynamic equilibrium which sets the

relationship between bundle diameter and concentration. If such a correlation exists here, the solvent volume per graphene flake should be proportional to the volume of the sphere defined by the flake length (see figure 1, lower inset, right). Then, we can relate the graphene concentration as proportional to the mass of the average flake divided by the volume of the associated sphere. In this scenario, the concentration is given by:

$$C_G \approx k\frac{\rho_G\langle L\rangle\langle w\rangle\langle N\rangle d}{4\pi\langle L/2\rangle^3/3} \approx k\frac{6\rho_G d}{\pi}\frac{\langle w\rangle\langle N\rangle}{\langle L\rangle^2} \propto \sqrt{t} \qquad (1)$$

Where k is the proportionality constant, ρ_G is the graphitic density (2200 kg m^{-3}) and d is the interlayer spacing (0.35 nm). In addition, equation 1 explains the observed scaling of C_G with $\sqrt{t}$. Given the invariance of $\langle N\rangle$ with time and the observed scaling of $\langle L\rangle$ and $\langle w\rangle$ with $t^{-1/2}$, the $\sqrt{t}$ dependence emerges naturally from equation 1. In fact, by inserting the fit formulae shown in figure 3 into equation 1, we can fit it to the data shown in figure 1. The dashed line in figure 1 is the fit to equation 1 and, rather surprisingly, gives k=1.0. This particular value of k is consistent with the situation where the concentration is such that each flake exactly occupies its spherical volume. This shows that the concentration and aggregation state interact to keep the system close to a critical concentration similar to the overlap concentration in polymer physics.[38]

This behaviour, described by k=1, is not general but represents the state of the system when the concentration is close to its maximum value (set by flake size as described above). We observe this behaviour because we apply a very low centrifugation rate (500 rpm). This rate was chosen as the lowest rotation rate preliminary experiments showed to remove all large aggregates (ie those visible optically). Thus, this scenario represents the maximum concentration of well dispersed flakes. Higher rotation rates would result in the removal of more material, leading to reduced concentrations and values of k<1.

2.4 Centrifugation dependence.

As described above, one can reduce the concentration by varying the centrifugation parameters; we would expect higher rotation rates to give lower concentrations. To test this, we chose one sonication time (146 hours) and prepared a number of dispersions by centrifugation at four different rates from 500 rpm to 4000 rpm. We measured the concentration of graphene in each case. This data is presented in **figure 4**. Here we see the concentration fall off monotonically with rotation rate, from 0.5 mg/ml for 500 rpm to 0.13 rpm for 4000 rpm. (The 500 rpm data does not quite match that presented in figure 1 because

these samples were made separately and so differ slightly from the previous results as described in section 2.1) We note that this decay does not scale as $(rpm)^{-2}$ as might be expected from centrifugation theory. It is also important to point out that this decay does not invalidate equation 1, rather it suggests that k is a function of rpm with k=1 representing the maximum value.

In the simplest case, we would expect smaller flakes to remain at higher rotation rates. To test this, we performed TEM analysis on samples prepared at all four rotation rates. The measured mean lengths, <L>, and widths, <w>, are shown in figure 4 inset. Both flake dimensions fell from $\langle L \rangle$=1.02±0.07 μm, $\langle w \rangle$=0.38±0.03 μm and $\langle N \rangle$=3.1 for the 500 rpm sample to $\langle L \rangle$=0.54±0.05 μm, $\langle w \rangle$=0.19±0.01 μm and $\langle N \rangle$=2.9 for the 4000 rpm sample. This clearly shows that only smaller flakes remain dispersed at longer centrifugation times.

2.5 Defect formation?

We have demonstrated a method to produce highly exfoliated graphene dispersions at reasonably high concentration. However, as this procedure requires sonication for long times, the possibility of defect formation must be considered. To test this we prepared thin films (~50nm) by filtering a number of graphene dispersions through porous alumina membranes. We measured Raman spectra for at least 20 different spots on each film before normalising and averaging the spectra. The resultant spectra for the 36 hrs and 192 hrs sonication films (500 rpm) and the 146 hrs sonication films (500 rpm and 4000 rpm) are shown in **figure 5**. Also shown is a spectrum of the graphite powder. Of note are three bands;[39] the D band (~1350 cm^{-1}), the G band (~1600 cm^{-1}) and the 2D band (~2700 cm^{-1}). The D band gives evidence of the presence of defects; either edges[40] or topological defects in the sheet. We note that the starting powder displays a small defect population. We can quantify the defect level by the D to G band intensity ratio, I_D/I_G. As shown in figure 5 (inset), I_D/I_G increases gradually from the powder value with increasing sonication time. In addition, we found that I_D/I_G increases smoothly with rpm.

An important question is whether we introduce basal plane defects or defects associated with new edges. As the flakes get smaller with time, the total edge length increases with time. This would be consistent with the data in figure 5 (inset). In addition, if edges are responsible for the defect content, we would expect I_D/I_G to increase with centrifugation rate. We found that I_D/I_G increase smoothly with rpm.

We can quantitatively test the idea that the defect population is dominated by the edge defects by noting that, for edge defects, I_D should scale with the flake edge length while I_G should scale with the flake area. Approximating the flakes as rectangular, this means the average Raman ratio should scale as $\langle I_D / I_G \rangle \propto \left[\langle L \rangle^{-1} + \langle w \rangle^{-1} \right]$. This is shown to be the case in **figure 6** for both the samples prepared for different sonication times and different rotation rates. It is interesting that both data sets fall roughly on the same straight line. We reiterate that this scenario is consistent with the hypothesis that the increase in I_D/I_G can be explained solely by the introduction of new edges as the sheets get cut. However, we cannot categorically rule out the possibility that basal plane defects are induced by sonication and that their formation is flake size dependant. If the flake size dependence of the basal plane defect formation rate was just right, this mechanism could result in the behaviour observed in figure 6. However, we feel that this second explanation is unlikely as it would require a very specific size dependence of the body defect formation rate. It is more probable that the observed defects are in fact associated with the edges and the bodies of the flakes are relatively defect free. This is an important issue and will be studied in more detail in a future paper. Given the behaviour displayed in figure 6 and the observed time dependences of $\langle L \rangle$ and $\langle w \rangle$, it can be shown that I_D/I_G should scale with $\sqrt{t}$. That this is approximately the case is illustrated by the dashed line in figure 5 (inset).

We can also consider the 2D band. The shape of this band is indicative of the number of layers per flake.[39, 41] For flakes thinner than ~5 layers, the Raman spectrum is considerably different from that of graphene. None of the 70 spectra measured for the thin films described above displayed graphite-like character. Rather, all spectra were consistent with flakes of 3-5 layers in good agreement with the TEM data.

2.6 Film formation

Access to high quality, high concentration graphene dispersions will facilitate a number of areas of research such as composite or film formation. We illustrate this by preparing thick, free-standing films from dispersions sonicated for a range of times. The films were prepared by vacuum filtering the dispersions onto porous membranes to give films ~40-80 μm thick with densities of 1200-1350 kg m^{-3} (and so porosities of 40-45%). We performed all measurements on as-produced films; no annealing, washing or post-treatment was performed. Raman measurements (not shown) were similar to those measured for thin films and were representative of few layer graphene. In all cases, the films displayed a shiny

metallic sheen as shown in **figure 7A**. This is similar to previously reported films of reduced graphene oxide.[10] Scanning electron microscopy of a film edge shows it to display a well defined layered morphology (figure 7 B&C). Even though the porosity is relatively high, the flakes making up the films appear reasonably well packed.

We measured the DC conductivity of the films to be relatively invariant with sonication time, with a mean conductivity of $1.8\pm0.1\times10^4$ S m^{-1}. This value is considerably lower than the conductivity of graphite (~1.5×10^5 S m^{-1}). We expect the reason for this is that carriers must cross many inter-sheet junctions as they pass through the material. It has recently been confirmed that such junctions limit the conductivity of nanotube films.[42] This conductivity compares well with free-standing films of reduced graphene oxide reported recently which displayed conductivities of up to 3.5×10^4 S m^{-1} (after annealing at 350C).[10, 43] However, we note that similar, reduced GO films prepared without annealing displayed conductivities of ~7000 S m^{-1}.[10, 43]

We also performed mechanical measurements on these films. We cut strips from each film and performed tensile testing. Mechanically robust films were only formed for sonication times above 50 hrs. Representative stress-strain curves are shown in figure 7D. For films prepared with sonication times >50 hrs, the Young's modulus ranged from ~5-11 GPa. The film strength as a function of sonication time is shown in figure 7E. For times <50 hrs, the strength is negligible; indeed these films were extremely delicate and very hard to remove from the filter. For longer times, the strength was 12-18 MPa. We note that these moduli and strength are lower than those reported for films of both GO[44] and reduced GO[43] probably due to the reduced inter-sheet stress transfer associated with the absence of oxides and an interfacial layer of residual NMP[25] rather than oxides. By analogy with polymer-nanotube composites, such a layer is likely to promote interfacial slippage.[45] We note that these films have strengths similar to nanotube films cast from NMP.[46]

2.7 Aqueous dispersions

Using the solvent NMP has a number of disadvantages, notably its high boiling point. For many applications, water would be a better solvent. However, the surface energy of water is too high for it to act as a solvent for graphene.[25] We note however that aqueous dispersions of reduced graphene oxide have been heavily diluted with organic solvents without large scale destabilisation.[17] With this in mind, we diluted an (homogenised by 10 min bath sonication) NMP dispersion (0.7 mg ml^{-1}, 2ml) with water by a factor of 99:1 (water:NMP). For comparison, we diluted the same starting dispersion with NMP at 99:1.

Each dispersion was then bath sonicated for a further 10 mins to homogenise. We measured the resulting sedimentation by tracking optical absorbance using a home built apparatus.[47] Sedimentation curves for both water and NMP diluted NMP dispersions are shown in **figure 8A**. Both samples were very stable over 160 hours showing <25% sedimentation. Each sedimentation could be well fit to an exponential decay[47] (see figure 8). Here the parameter A_0 represents the fraction of graphene stable against sedimentation. This was A_0~80% for the NMP sample, falling to A_0~70% for the water diluted sample. This stability against sedimentation when exposed to a non-solvent (water) is not understood but will be very useful for many applications as long as signification aggregation does not occur. To test this we carried out TEM analysis on the dispersions immediately after dilution. In both cases mono- and multi-layers were observed. An example of graphene flakes observed in the water diluted sample is shown in figure 8 inset. Shown in figure 8B and C are statistical data for the flake thickness in the NMP and water diluted samples respectively. While the water diluted sample has fewer monolayers, the exfoliation state is still reasonably good.

3.0 Conclusion

In conclusion we have demonstrated a method to prepare dispersions of graphene in NMP at concentrations of up to 1.2 mg ml^{-1} by extended sonication. The flake dimensions decrease with sonication time as $t^{-1/2}$, while the concentration is directly related to the flake size. The intensity of the Raman D band increases with time as $t^{1/2}$, indicating that new edges rather than basal plane defects are formed. Dilution with water causes little aggregation or sedimentation. These dispersions can be formed into free standing films with reasonable mechanical and electrical properties. We believe this method will greatly facilitate the preparation of materials such as composites or transparent films.

4.0 Experimental Section

A set of identical graphene dispersions were prepared by adding powdered graphite (Branwell natural graphite, grade 2369, www.branwell.u-net.com/) to N-methyl-pyrrolidone (NMP) (spectroscopic grade, Aldrich) at a concentration of 3.3 mg ml^{-1} (700 ml, round bottomed flask). These dispersions were then sonicated (Branson 1510E-MT bath sonicator) for various periods from 0.5 hrs to 462 hrs. During sonication over such a prolonged period, the bath water tends to heat up to ~50C and considerable evaporation occurs. To combat this, a siphon system must be used to allow water to flow from a reservoir to keep the water level constant. We note that the true power output (estimated from the measured rate of temperature

increase (K s^{-1}) when sonicating a known mass of water) tends to vary between (even nominally identical) sonic baths. In this work, we used one bath which had a measured power output of 23W. If significantly higher power baths are used, the bath-water tends to heat significantly, degrading the solvent and resulting in poorer results. After sonication, the dispersions were transferred to vials and centrifuged at 500rpm for 45 minutes (Hettich Mikro 22R) (500-4000 rpm for the centrifugation rate experiment). After centrifugation, the top 20ml (out of 28 ml) was carefully removed and retained for further use.

UV-vis-IR absorption spectroscopy was carried out using a Varian Cary6000i (l=1mm cuvette). Samples for TEM were prepared by pipetting a few milliliters of dispersion onto holey carbon grids (400 mesh). Bright field TEM images were taken with a Jeol 2100 operating at 200 kV. Thin films were prepared using porous alumina membranes (Whatman Anodisc 47mm, pore size =0.02μm). Raman spectra (633 nm) were recorded on a Horiba Jobin Yvon LabRAM-HR (100× objective lens). Thick films were prepared by vacuum filtering the dispersions onto porous membranes to give films ~40-80 μm thick. They were dried for 24hrs in a 65 C oven followed by 48hrs in a vac oven at 60 C. Tensile tests were carried out using a Zwick Roell with 100 N load cell at a strain rate of 100 mm/min.

Acknowledgements

We acknowledgement financial support from Science Foundation Ireland. A O'N and ML thank IRCSET for financial support. (Supporting Information is available online from Wiley InterScience or from the author).

Received: ((will be filled in by the editorial staff))

Revised: ((will be filled in by the editorial staff))

Published online: ((will be filled in by the editorial staff))

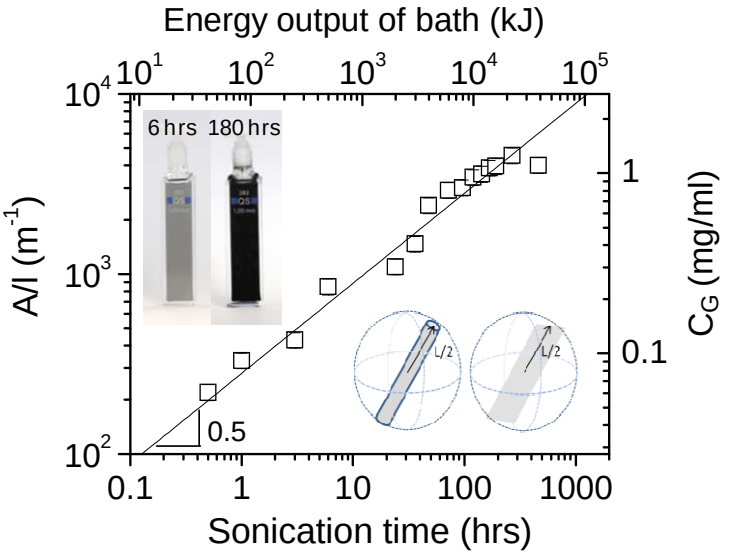

Figure 1. Concentration of graphene after centrifugation as a function of sonication time. On the left axis is the measured absorbance per cell length, A/l, while on the right axis is the concentration calculated using an absorption coefficient of 3620 ml mg^{-1} m^{-1}. The line illustrates √t behaviour and is a fit to equation 1. The upper axis shows the total energy outputted by the bath calculated using the measured power output of 23 W. The upper inset shows 1mm cuvettes containing dispersions after 6 and 180 hrs. The lower inset illustrates the hypothesis that the concentration of both nanotube and graphene dispersions is determined by the volume of the solvent sphere defined by the tube or flake dimensions.

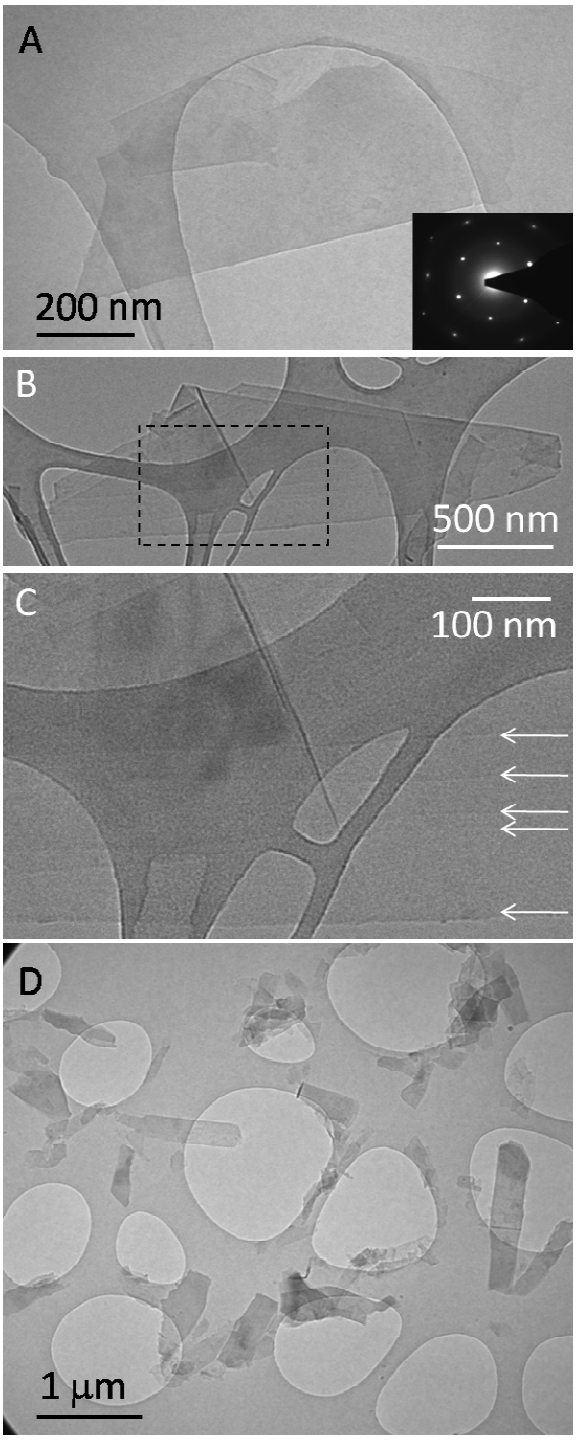

Figure 2. TEM images of graphene flakes observed during this work. A) A typical monolayer, inset: A diffraction pattern taken from a monolayer. B) A multilayer C) a magnified version of the portion of B in the dashed box. The arrows in this image show the position of the edges of the individual flakes comprising this multilayer. Five edges can be seen showing that this is a 5-layer flake. D) A widefield image showing the large quantities of flakes observed after long sonication times (180 hrs)

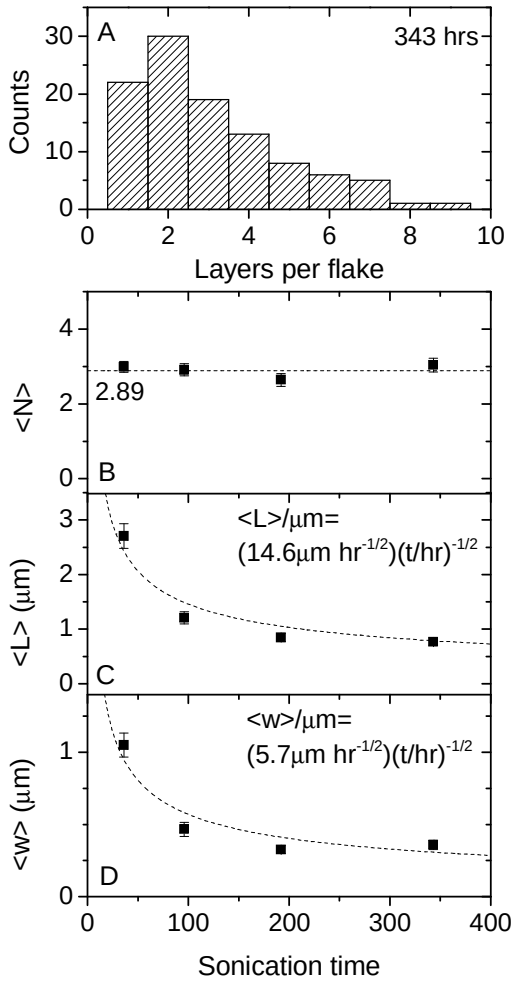

Figure 3. A) Histogram showing the number of layers per flake measured for the 343 hr sonication times. B) Mean number of layers per flake. C) and D) Mean length and width of flakes respectively. Note that both flake length and width scale well with the inverse square root of time ($t^{-1/2}$).

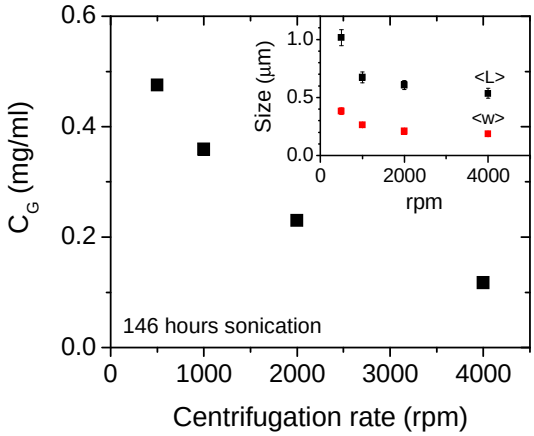

Figure 4. Concentration of graphene as a function of centrifugation rate for a constant sonication time of 146 hours. Inset: Flake size as a function of sonication time.

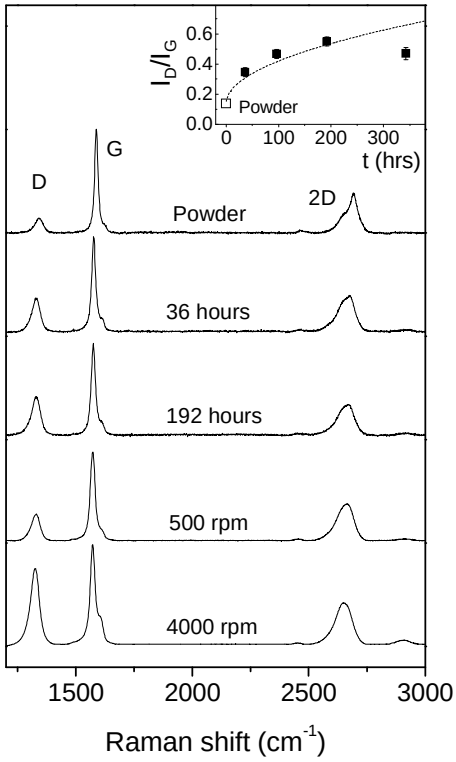

Figure 5. Raman spectra of starting graphite powder and of thin filtered films prepared after 36 and 192 hrs sonication (500 rpm) and after 146 hours sonication but centrifuged with rates of 500 rpm and 4000 rpm. Inset: The ratio of D band to G band intensity as a function of sonication time. The errors are standard errors of the distribution of >20 I_D/I_G values. The

dashed line shows the behaviour expected if the change in D band intensity is due to edge formation.

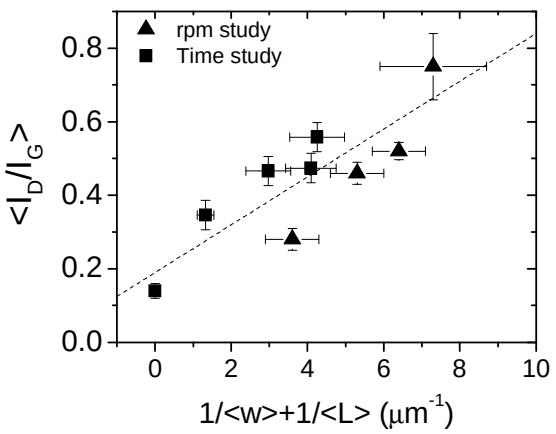

Figure 6: Mean Raman D:G ratio as a function of edge length to flake area ratio, $\langle w\rangle^{-1}+\langle L\rangle^{-1}$. If the D band increase is due to the formation of new flake edges, a straight line would be expected in this graph. The errors in $\langle I_D/I_G\rangle$ are standard errors of the distribution of >20 I_D/I_G values while the errors in $\langle w\rangle^{-1}+\langle L\rangle^{-1}$ are calculated from the standard errors of the flake length and width distributions. Note that the data point at the bottom left of this graph represents the graphite powder.

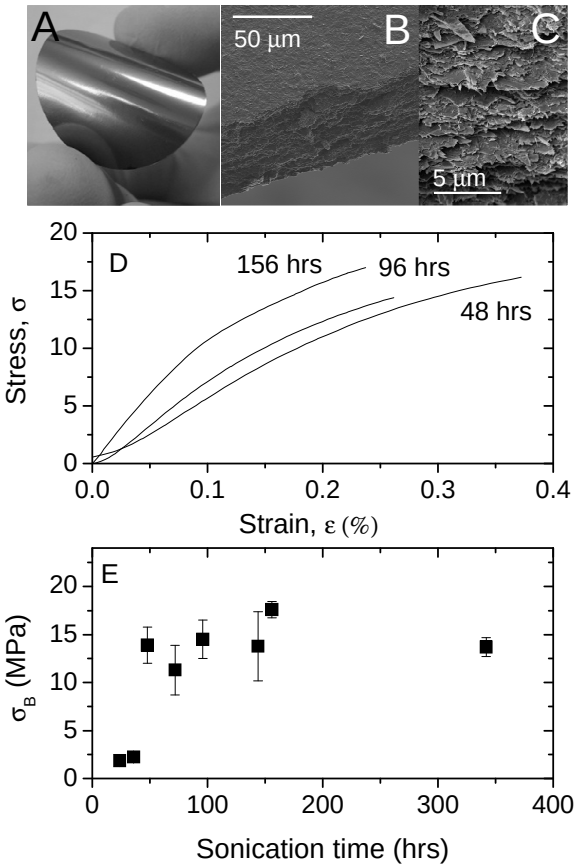

Figure 7. A) A photograph of a free standing film prepared from a 96 hr sample. B) SEM image of the edge of the film in A). C) Close up of B). D) Representative stress-strain curves for a number of films studied. E) Ultimate tensile strength of films as a function of sonication time.

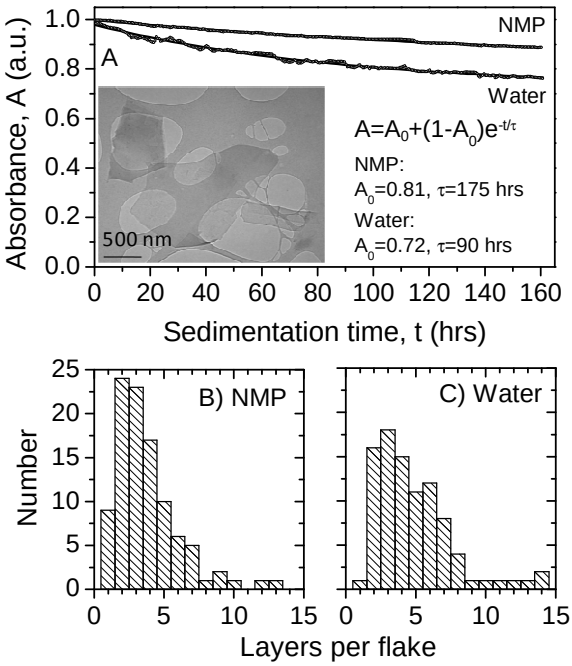

Figure 8: A) sedimentation behaviour for graphene dispersions (diluted from 0.7 mg/ml to 0.007 mg/ml) by addition of either NMP or water. Each curve fits well to an exponential decay described by the parameters shown. Inset: A TEM image of a graphene monolayer from the water dilution. TEM statistics showing the aggregation state of the dispersion diluted with B) NMP and C) water.

TOC Graphic

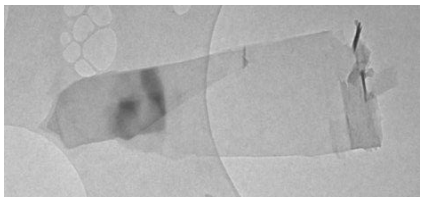

A graphene flake deposited from a 99:1 water:NMP dispersion.

References

[1] C. Lee, X. D. Wei, J. W. Kysar, J. Hone, *Science* **2008**, *321*, 385.
[2] K. S. Novoselov, A. K. Geim, S. V. Morozov, D. Jiang, Y. Zhang, S. V. Dubonos, I. V. Grigorieva, A. A. Firsov, *Science* **2004**, *306*, 666.
[3] A. A. Balandin, S. Ghosh, W. Z. Bao, I. Calizo, D. Teweldebrhan, F. Miao, C. N. Lau, *Nano Letters* **2008**, *8*, 902.
[4] A. K. Geim, K. S. Novoselov, *Nature Materials* **2007**, *6*, 183.
[5] A. K. Geim, *Science* **2009**, *324*, 1530.
[6] K. S. Novoselov, D. Jiang, F. Schedin, T. J. Booth, V. V. Khotkevich, S. V. Morozov, A. K. Geim, *Proceedings of the National Academy of Sciences of the United States of America* **2005**, *102*, 10451.
[7] R. Ruoff, *Nature Nanotechnology* **2008**, *3*, 10.
[8] S. Stankovich, D. A. Dikin, G. H. B. Dommett, K. M. Kohlhaas, E. J. Zimney, E. A. Stach, R. D. Piner, S. T. Nguyen, R. S. Ruoff, *Nature* **2006**, *442*, 282.
[9] S. Stankovich, R. D. Piner, X. Q. Chen, N. Q. Wu, S. T. Nguyen, R. S. Ruoff, *Journal of Materials Chemistry* **2006**, *16*, 155.
[10] D. Li, M. B. Muller, S. Gilje, R. B. Kaner, G. G. Wallace, *Nature Nanotechnology* **2008**, *3*, 101.
[11] I. Jung, M. Pelton, R. Piner, D. A. Dikin, S. Stankovich, S. Watcharotone, M. Hausner, R. S. Ruoff, *Nano Letters* **2007**, *7*, 3569.
[12] I. Jung, M. Vaupel, M. Pelton, R. Piner, D. A. Dikin, S. Stankovich, J. An, R. S. Ruoff, *Journal of Physical Chemistry C* **2008**, *112*, 8499.
[13] X. Wang, L. J. Zhi, K. Mullen, *Nano Letters* **2008**, *8*, 323.
[14] J. B. Wu, H. A. Becerril, Z. N. Bao, Z. F. Liu, Y. S. Chen, P. Peumans, *Applied Physics Letters* **2008**, *92*, 263302.
[15] S. Stankovich, D. A. Dikin, R. D. Piner, K. A. Kohlhaas, A. Kleinhammes, Y. Jia, Y. Wu, S. T. Nguyen, R. S. Ruoff, *Carbon* **2007**, *45*, 1558.
[16] I. Jung, D. A. Dikin, R. D. Piner, R. S. Ruoff, *Nano Letters* **2008**, *8*, 4283.
[17] S. Park, J. H. An, I. W. Jung, R. D. Piner, S. J. An, X. S. Li, A. Velamakanni, R. S. Ruoff, *Nano Letters* **2009**, *9*, 1593.
[18] H. A. Becerril, J. Mao, Z. Liu, R. M. Stoltenberg, Z. Bao, Y. Chen, *Acs Nano* **2008**, *2*, 463.
[19] S. De, P. J. King, M. Lotya, A. O'Neill, E. M. Doherty, Y. Hernandez, G. S. Duesberg, J. N. Coleman, *Small* **2009**, *DOI: 10.1002/smll.200901162*
[20] G. Eda, G. Fanchini, M. Chhowalla, *Nature Nanotechnology* **2008**, *3*, 270.
[21] C. Gomez-Navarro, R. T. Weitz, A. M. Bittner, M. Scolari, A. Mews, M. Burghard, K. Kern, *Nano Letters* **2007**, *7*, 3499.
[22] H. Kang, A. Kulkarni, S. Stankovich, R. S. Ruoff, S. Baik, *Carbon* **2009**, *47*, 1520.
[23] K. N. Kudin, B. Ozbas, H. C. Schniepp, R. K. Prud'homme, I. A. Aksay, R. Car, *Nano Letters* **2008**, *8*, 36.
[24] D. Yang, A. Velamakanni, G. Bozoklu, S. Park, M. Stoller, R. D. Piner, S. Stankovich, I. Jung, D. A. Field, C. A. Ventrice, R. S. Ruoff, *Carbon* **2009**, *47*, 145.
[25] Y. Hernandez, V. Nicolosi, M. Lotya, F. M. Blighe, Z. Y. Sun, S. De, I. T. McGovern, B. Holland, M. Byrne, Y. K. Gun'ko, J. J. Boland, P. Niraj, G. Duesberg, S. Krishnamurthy, R. Goodhue, J. Hutchison, V. Scardaci, A. C. Ferrari, J. N. Coleman, *Nature Nanotechnology* **2008**, *3*, 563.

[26] M. Lotya, Y. Hernandez, P. J. King, R. J. Smith, V. Nicolosi, L. S. Karlsson, F. M. Blighe, S. De, Z. M. Wang, I. T. McGovern, G. S. Duesberg, J. N. Coleman, *Journal of the American Chemical Society* **2009**, *131*, 3611.
[27] A. B. Bourlinos, V. Georgakilas, R. Zboril, T. A. Steriotis, A. K. Stubos, *Small* **2009**, *5*, 1841.
[28] P. Blake, P. D. Brimicombe, R. R. Nair, T. J. Booth, D. Jiang, F. Schedin, L. A. Ponomarenko, S. V. Morozov, H. F. Gleeson, E. W. Hill, A. K. Geim, K. S. Novoselov, *Nano Letters* **2008**, *8*, 1704.
[29] A. A. Green, M. C. Hersam, *Nano Letters* **2009**, *In press, DOI 10.1021/nl902200b*.
[30] J. R. Lomeda, C. D. Doyle, D. V. Kosynkin, W. F. Hwang, J. M. Tour, *Journal of the American Chemical Society* **2008**, *130*, 16201.
[31] V. C. Tung, M. J. Allen, Y. Yang, R. B. Kaner, *Nature Nanotechnology* **2009**, *4*, 25.
[32] G. Williams, B. Seger, P. V. Kamat, *Acs Nano* **2008**, *2*, 1487.
[33] S. Park, J. H. An, R. D. Piner, I. Jung, D. X. Yang, A. Velamakanni, S. T. Nguyen, R. S. Ruoff, *Chemistry of Materials* **2008**, *20*, 6592.
[34] S. Park, R. S. Ruoff, *Nature Nanotechnology* **2009**, *4*, 217.
[35] F. Hennrich, R. Krupke, K. Arnold, J. A. Rojas Stutz, S. Lebedkin, T. Koch, T. Schimmel, M. M. Kappes, *The Journal of Physical Chemistry B* **2007**, *111*, 1932.
[36] S. Giordani, S. D. Bergin, V. Nicolosi, S. Lebedkin, M. M. Kappes, W. J. Blau, J. N. Coleman, *Journal of Physical Chemistry B* **2006**, *110*, 15708.
[37] S. D. Bergin, V. Nicolosi, P. V. Streich, S. Giordani, Z. Y. Sun, A. H. Windle, P. Ryan, N. P. P. Niraj, Z. T. T. Wang, L. Carpenter, W. J. Blau, J. J. Boland, J. P. Hamilton, J. N. Coleman, *Advanced Materials* **2008**, *20*, 1876.
[38] M. Rubinstein, R. H. Colby, *Polymer Physics*, Oxford University Press, Oxford **2003**.
[39] A. C. Ferrari, J. C. Meyer, V. Scardaci, C. Casiraghi, M. Lazzeri, F. Mauri, S. Piscanec, D. Jiang, K. S. Novoselov, S. Roth, A. K. Geim, *Physical Review Letters* **2006**, *97*.
[40] C. Casiraghi, A. Hartschuh, H. Qian, S. Piscanec, C. Georgi, A. Fasoli, K. S. Novoselov, D. M. Basko, A. C. Ferrari, *Nano Letters* **2009**, *9*, 1433.
[41] L. M. Malard, M. A. Pimenta, G. Dresselhaus, M. S. Dresselhaus, *Physics Reports-Review Section of Physics Letters* **2009**, *473*, 51.
[42] P. N. Nirmalraj, P. E. Lyons, S. De, J. N. Coleman, J. J. Boland, *Nano Letters* **2009**, *in press, DOI 10.1021/nl9020914*.
[43] H. Chen, M. B. Muller, K. J. Gilmore, G. G. Wallace, D. Li, *Advanced Materials* **2008**, *20*, 3557.
[44] D. A. Dikin, S. Stankovich, E. J. Zimney, R. D. Piner, G. H. B. Dommett, G. Evmenenko, S. T. Nguyen, R. S. Ruoff, *Nature* **2007**, *448*, 457.
[45] U. Khan, K. Ryan, W. J. Blau, J. N. Coleman, *Composites Science and Technology* **2007**, *67*, 3158.
[46] F. M. Blighe, P. E. Lyons, S. De, W. J. Blau, J. N. Coleman, *Carbon* **2008**, *46*, 41.
[47] V. Nicolosi, D. Vrbanic, A. Mrzel, J. McCauley, S. O'Flaherty, C. McGuinness, G. Compagnini, D. Mihailovic, W. J. Blau, J. N. Coleman, *Journal of Physical Chemistry B* **2005**, *109*, 7124.

Supporting Information

High concentration solvent-exfoliation of graphene

By *Umar Khan, Arlene O'Neill, Mustafa Lotya, Sukanta De,* and *Jonathan N Coleman* *

[*] Prof. J. N. Coleman, Dr. S. De, Dr U. Khan, Mr M. Lotya, Ms. A. O'Neill
School of Physics and CRANN
Trinity College Dublin,
Dublin 2 (Ireland)
E-mail: (colemaj@tcd.ie)

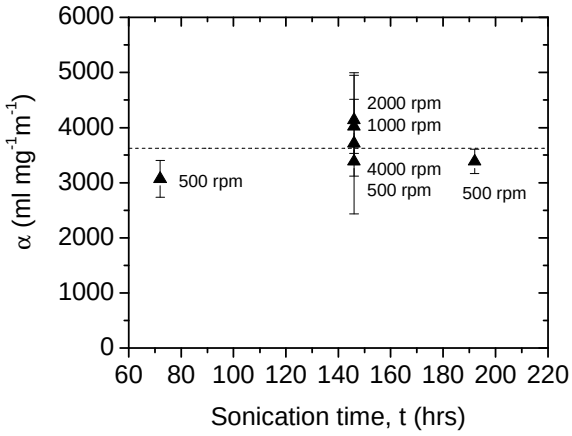

Figure S1: Absorption coefficient , α,of graphene dispersions as a function of sonication time and centrifugation rate. The absorption coefficient is relatively invariant, displaying a mean of 3620 ml mg^{-1} m^{-1}.

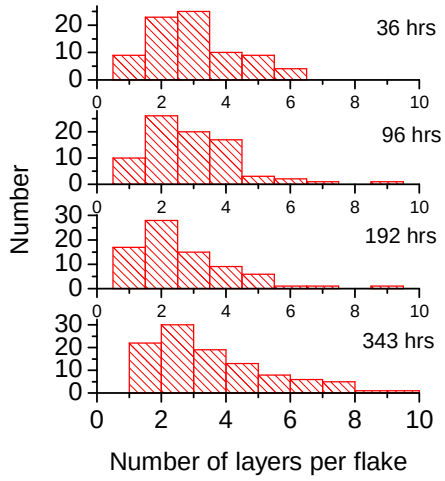

Figure S2: Histograms showing the number of layers per flake measured for a number of sonication times. Note that monolayers were observed in all cases.

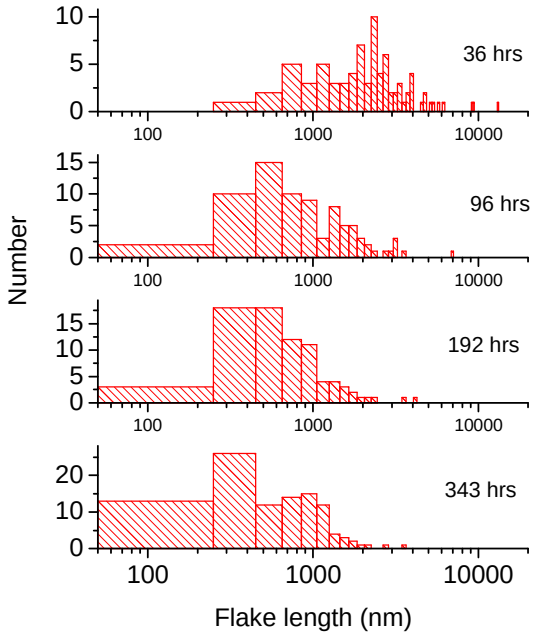

Figure S3: Histograms of the length of graphene flakes observed by TEM as a function of sonication time.

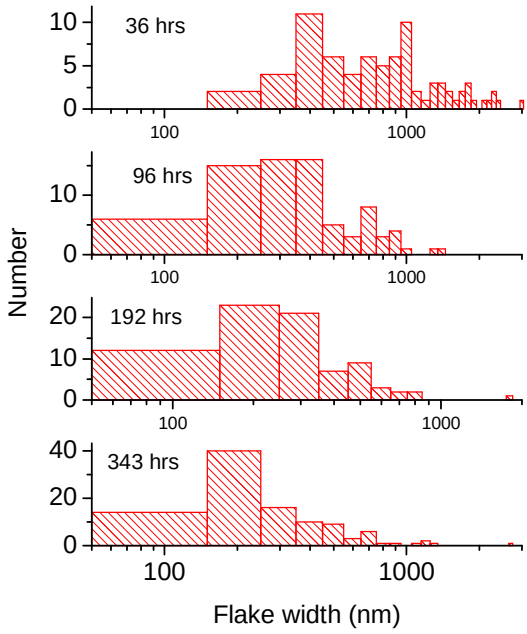

Figure S4: Histograms of the width of graphene flakes observed by TEM as a function of sonication time.

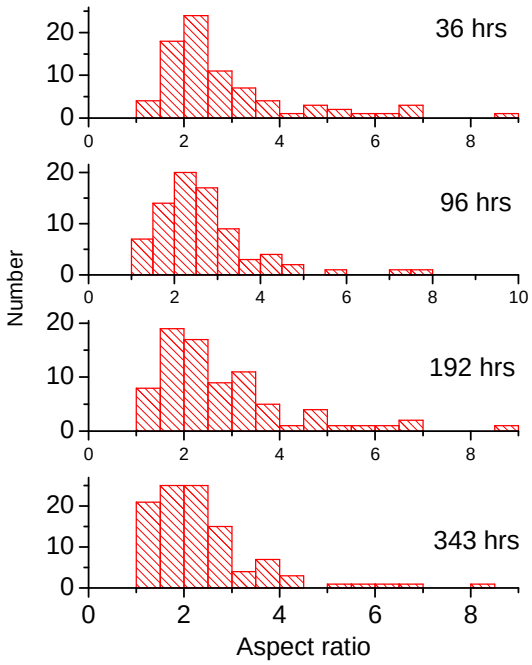

Figure S5: Histograms of the aspect ratio of graphene flakes observed by TEM as a function of sonication time.

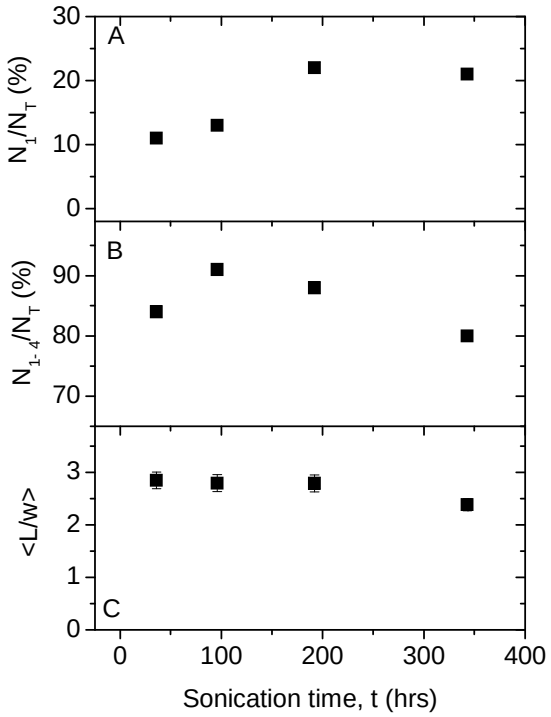

Figure S6: Statistical data derived from the histograms in figures S1-4, plotted in all cases as a function of sonication time. A) Fraction of monomers, N_1/N_T. B) Fraction of flakes with less than 5 layers, N_{1-4}/N_T. C) Average flake aspect ratio, <L/w>. All error bars represent standard errors.